Indian journal of
Engineering

Solar water pumping: Experimental evaluation of the Buck converter effect under low irradiance conditions

Hachemi Ammar[1*], Noureddine Benbaha[1], Mohamed Tewfik Bouziane[2]

To Cite:
Ammar H, Benbaha N, Bouziane MT. Solar water pumping: Experimental evaluation of the Buck converter effect under low irradiance conditions. *Indian Journal of Engineering*, 2025, 22, e8ije1695
doi: https://doi.org/10.54905/disssi.v22i57.e8ije1695

Author Affiliation:
[1]Unité de Recherche Appliquée en Energies Renouvelables, URAER, Centre de Développement des Energies Renouvelables, CDER, 47133, Ghardaïa, Algeria
[2]Mohamed Khider University, BP 145 RP, 07000 Biskra, Algeria

[*]Corresponding Author:
Hachemi Ammar
Unité de Recherche Appliquée en Energies Renouvelables, URAER, Centre de Développement des Energies Renouvelables, CDER, 47133, Ghardaïa, Algeria. Email: hachemi.ammar@gmail.com

Peer-Review History
Received: 27 November 2024
Reviewed & Revised: 07/December/2024 to 03/April/2025
Accepted: 12 April 2025
Published: 21 April 2025

Peer-Review Model
External peer-review was done through double-blind method.

Indian Journal of Engineering
pISSN 2319–7757; eISSN 2319–7765

DISCOVERY SCIENTIFIC SOCIETY

ABSTRACT

A stand-alone solar water pumping system is an excellent solution, especially for remote locations. In such systems, solar energy is captured directly from photovoltaic panels without using battery storage or any type of energy conversion. The energy is then stored as hydraulic energy in a reservoir to be used later for purposes such as the irrigation of agricultural crops. These systems have a unique characteristic in that the operational parameters of the pumps, such as total dynamic head (TDH), flow rate, and efficiency, depend on solar irradiation, which changes with the season and across the day. The results show that in the daytime, when solar radiance is low at sunrise and sunset, the pump cannot reach the fixed head. Low solar radiance conditions have led to several ideas for pumping system adjustments. The selected solution noticeably increases the water pumped in these conditions.

Keywords: Photovoltaic, Pumping, Experimental evaluation, Direct-coupled, Buck converter

1. INTRODUCTION

Solar-powered water pumping systems are becoming increasingly crucial in off-grid and remote places to help solve global water and energy problems. These systems have changed agriculture because they make it possible to water fields efficiently without using expensive diesel generators or energy from the power grid. Farmers in arid and semi-arid areas today use solar-powered pumps to access groundwater, thus enabling year-round crop production and lowering vulnerability to drought (Kumar et al., 2023). DC-DC converter is an essential component of these systems since it improves the performance of the solar-powered pump by changing voltage and increasing power transmission from the photovoltaic (PV) panels. DC-DC converters change to match changing solar irradiation and temperature conditions using MPPT (Maximum Power Point Tracking) algorithms, ensuring maximum system efficiency. This ability greatly increases water pumping efficiency, lowers energy losses, and extends the system's lifetime (Girgis & Elkhateeb, 2024).

Also, high-tech DC-DC converters make the system more stable and compatible, which makes it easier to combine different kinds of photovoltaic panels and pump motors. Community water supply initiatives, particularly in areas with limited access to drinking water, use solar-powered water pumping devices in addition to agriculture. Non-governmental organizations and governments in countries across Africa, Asia, and Latin America have adopted solar pumping solutions to provide potable water to underserved populations, enhancing public health and reducing the water-collecting load on children and women (Durga et al., 2024).

Solar water pumps are being included in wastewater treatment plants for industrial uses, where they contribute to water recycling and purification using sustainable energy. Moreover, these systems have been included in disaster relief initiatives to provide clean water in times of crisis, such as following natural disasters when infrastructure is usually destroyed (Crovella et al., 2024). Emerging technologies, including intelligent solar-powered water pumping systems using Internet of Things (IoT) technology, have raised efficiency by enabling remote monitoring and real-time performance optimization. These advances have made solar-powered water pumps necessary for sustainable water management strategies and climate adaptation (Ramli & Jabbar, 2022). Adjusting the output voltage of solar panels (PV) requires DC-DC converters, guaranteeing fit with water pump motor requirements. The generation of solar power changes with variations in solar intensity, temperature, and meteorological conditions.

These fluctuations without a DC-DC converter may result in less-than-ideal pump performance or possible motor damage. Maintaining a constant voltage—which is crucial for sensitive applications like irrigation and potable water distribution—converters ensure stable and safe operation. Modern DC-DC converters are essentially capable of running MPPT algorithms. Maximum power point tracking ensures that the photovoltaic system operates at its maximum power output, irrespective of the ambient environmental conditions (Liou et al.., 2008; Haque, 2014). This feature is critical in solar pumping systems since it allows the system to maximize energy extraction from the photovoltaic panels even in cases of reduced light or shading. This improves general energy efficiency and lessens the need for large-scale solar panels (Benbaha et al., 2018).

DC-DC converters increase the energy flow between the solar panels and the pump motor, reducing power losses. Compared to simpler systems that might suffer efficiency loss from voltage or power fluctuations, transformers actively control voltage and current to maintain the best compatibility. In locations with limited access to solar energy, this efficiency especially helps to maximize water output per unit of solar energy (Nisha & Sheela, 2020). Solar water pumping systems often need to operate during early mornings, late afternoons, or cloudy days when solar irradiance is low. DC-DC converters allow the system to function effectively under such conditions by stepping up or stepping down the voltage as needed. This ensures continuous water supply even during suboptimal sunlight hours, which is critical for applications like livestock watering or irrigation (Muralidhar & Rajasekar, 2021; Farhat & Barambones, 2024). There are many kinds of modern DC-DC converters for use in IoT and creative technology. They assist the operators in monitoring performance data, finding problems remotely, and changing settings for the right functionality. It offers real-time monitoring and regulation of the solar water pumping system. Through means of data on water demand, solar energy availability, and pump efficiency, one can improve energy consumption and reduce waste (Angadi et al., 2021; Kassakian et al., 2023; Sutikno et al., 2023; Raj et al., 2020).

Solar energy is usually utilized directly from photovoltaic panels in stand-alone water pumping systems, without using battery storage or any type of energy conversion. The only option to store energy for later use, such as agricultural irrigation, is in the form of hydropotential energy. The uniqueness of these systems is that the characteristics of the used pumps (flow rate, TDH, and efficiency) are dependent firmly on solar radiance, which varies throughout the day and year, thus affecting consequently the operation point of the pump (Alkuhayli et al, 2024; Ammar et al, 2012; Ammar et al, 2014).

Our study is divided into two main phases in this paper. In the first phase, we characterize DC pumps (Shurflo 9325 model) in our laboratory's experimental test bench to evaluate their performance. After analyzing the results, we can identify times of low pump efficiency during the day. Under the second phase, we try to enhance the pump's efficiency in low-solar-radiance circumstances. We carry out the process as before, except we use a buck converter to derive power from solar panels. Pump efficiency and daily water pumped show a notable increase, thanks to the used strategy. The main objective of this work is to modify the pump's efficiency during the day, mostly in low solar radiation. This strategy significantly affects the daily water pump output to satisfy the agricultural demand.

2. PUMPING BENCH TEST SETUP

Testing the solar pumping system on the experimental bench at URAER (Applied Research Unit for Renewable Energies Ghardaia), where the pumping process is carried out in a closed loop out of stainless steel. The control valve keeps the target head fixed, as Figure 1 shows. Figure 1 depicts the main components of this system:

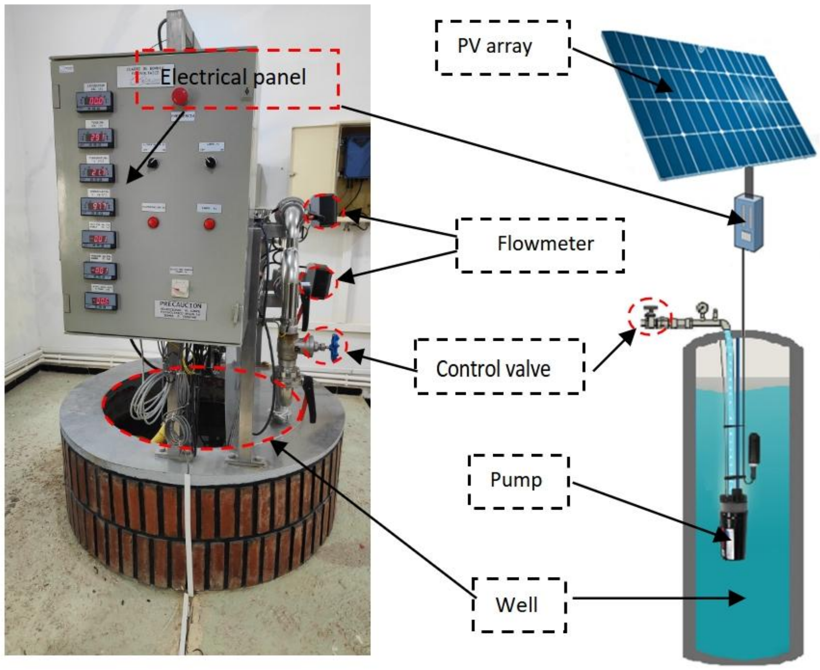

Figure 1 Solar pumping test bench

Solar modules

The Isofoton manufactured the monocrystalline silicon solar modules used for the pump tests, which had 110W of peak power output (Table 1). The PV panel arrangements are dependent on the pump test.

Table 1 Electrical characteristics of PV module (Isofoton 110w)

	Parameter	Value
Isofoton 110 W	Maximum Power point Maximum Voltage Maximum Current Isc V_{OC} muIsc Active Module area Panel Efficiency	110 W 34.8 V 3.16 A 3.38 A 43.2 V 2.3 mA/°C 0.75 m² 12.9%

Tank

As an artificial well, we use a tank of stainless steel with a depth of 02 meters.

Measuring instruments and equipment

a) Two electromagnetic flowmeters have been set to track daily water consumption and measure flow rate.
b) Two pressure transducers are installed, one for high pressure and the other for low pressure to measure pressure levels and determine the TDH of the pump (Total dynamic head).
c) A throttling valve (control valve) is used to adjust the system pressure, enabling the simulation of the pump’s dynamic head under varying conditions.
d) The global irradiance measurements were taken using a solar sensor, which is a silicon sensor.
e) Voltage and current sensors are also included in the electrical panel for control and display.

Data acquisition

An Agilent 34970A data logger recorded and stored data on a computer for later study and evaluation.

Pump

Shurflo designed and produced the pump used in this test, especially the 9325 model. Table 2 summarizes the pump's technical specifications.

Table 2 Technical specifications of the pump

Shurflo 9325		
Pump	Model number	9325-043-101
	Pump design	Positive displacement diaphragm pump
	Materials	High strength plastics stainless steel hardware
	Maximum head	70 m
	Maximum submersion	30 m
	Dimensions	305 mm x 395 mm
	Weight	2.72 kg
Motor	Motor type	Permanent Magnet Thermally protected
	Nominal voltage	24 VDC
	Nominal power	120 W
	Maximum amperage	4 A

3. METHODOLOGY

This paper is divided into two phases in our study. The system is compared to certain pump behavior (DC pump characterization) previously obtained (Shurflo 9325 type) in our experimental test bench (Figure 1) at the laboratory in responding to the performance metrics. The pump is supplied by a 24V and a 100 W photovoltaic module. We deploy the gate valve located at the circuit's output to regulate the pump's flow rate and total dynamic head (TDH).

The second phase increases the pump's effectiveness under low solar irradiation circumstances. Except for using a buck converter for power supply from solar panels, we continue with the same manipulation as the first one (Figure 2). The acquired data will be analyzed rigorously to identify all factors influencing the pump's TDH.

Figure 2. Buck converter and pump used

Buck converter functioning mode

A buck converter is a switch-mode DC-to-DC electronic converter, sometimes known as a step-down converter. The output voltage, sometimes called the load, is adjusted to be below the supply voltage. It typically includes at least two semiconductors (such as a MOSFET and a diode) and at least one energy storage element, such as a capacitor, inductor, or both (Figure 3). To eliminate voltage ripple, capacitor filters are most often connected to the input and output of this type of converter (load-side filter and supply-side filter). The pump represents the load in our scenario, while the PV panel is the energy source. In addition to controlling the performance optimization of the pumping system, the controller also serves as the pump's protector.

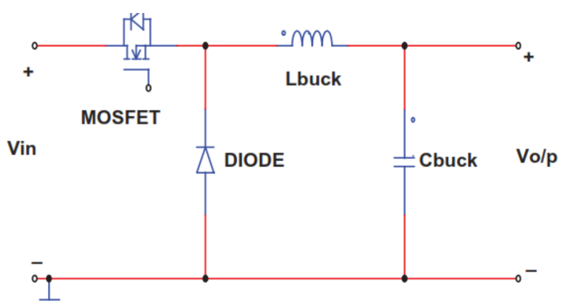

Figure 3 Buck converter circuit diagram

4. RESULTS AND DISCUSSION

Several manipulations were done during the day; the obtained refer to the instantaneous solar radiation (E)، Total Dynamic Head (TDH), instantaneous flow rate (Q), current (I), voltage (V) and P_out (w).

Analyze of the accuracy and reliability of experimental data

Scientific research, engineering, and decision-making rest on the accuracy and reliability of experimental data validation as much as they do on experimental design. It ensures correct results, supports wise decisions, and conserves a good reputation.

Data preparation

To accomplish this critical step, we use two datasets:

• The file My_data.csv contains our experimental data.

• The file my_data.csv holds the benchmark data.

We read both files with the help of Pandas, a Python library that helps in dealing with any wrong or missing data comfortably.

Descriptive statistics

Descriptive statistics of data is an important step because it concisely summarizes data in a clear manner, bringing out trends, patterns, central tendency, and variability features necessary for proper understanding and interpretation of datasets.

For both datasets, we calculate:

- Mean
- Median
- Standard deviation
- Coefficient of variation

The Coefficient of Variation (CV) is expressed as a percentage:

$$CV = \frac{\sigma_x}{\mu_x} \times 100 \quad (1)$$

Where σ is the standard deviation of x point and μ is the mean.

The table 3 summarizes the results of the description statistics.

Table 3: Summary of statistics of descriptive

Column	Dataset	Mean	Median	Std	Min	Max	CV (%)
Current	Experimental	1.93	1.94	0.40	1.06	2.73	20.74
Current	Benchmark	1.83	1.74	0.43	1.06	2.92	23.27
Voltage	Experimental	25.60	24.37	4.79	16.45	33.79	18.72
Voltage	Benchmark	28.66	30.06	5.44	9.51	35.91	18.97
P_out	Experimental	48.17	47.29	7.63	34.34	65.61	15.84
P_out	Benchmark	51.89	51.99	13.53	11.11	79.34	26.08
TDH	Experimental	19.14	19.77	9.48	0.09	36.85	49.53
TDH	Benchmark	16.30	15.03	9.19	0.31	41.86	56.39
Flow rate	Experimental	0.22	0.18	0.17	0.00	1.24	78.80
Flow rate	Benchmark	0.33	0.35	0.16	0.00	1.14	48.21

Accuracy metrics

To evaluate data accuracy, we have opted for the following parameters:

- The Mean absolute error (MAE)
- The Root mean square error (RMSE)
- Pearson correlation coefficient (r)
- Bias

To define the nature of the relationship between two variables, we usually measure the Pearson Correlation Coefficient (r). It gives us the direction and strength of the relationship. It is determined using the covariance of the variables divided by their standard deviations:

$$r = \frac{\sum(x_i - \mu_X)(y_i - \mu_Y)}{\sqrt{\sum(x_i - \mu_X)^2 \sum(y_i - \mu_Y)^2}} \quad (2)$$

Reliability metrics

To evaluate data reliability, we have opted for the following parameters:

- Coefficient of Variation (cv)

For the coefficient of variation, we apply formula 1.

- Signal-to-Noise Ratio (SNR):

The signal-to-noise ratio (SNR) is used to measure the strength of a desired signal relative to background noise. It is determined using the ratio of the mean to the standard deviation of the noise:

$$SNR = \frac{\sigma_X}{\mu_X} \quad (3)$$

Table 4 summarizes the results of the accuracy and the reliability analysis

Table 4 Accuracy and reliability metrics

Column	MAE	RMSE	Pearson Correlation Coefficient (r)	Bias	CV	SNR
Current	0.56	0.70	-0.22	0.46	20.74	4.82
Voltage	7.64	8.66	-0.12	-1.57	18.72	5.34
P_out	14.63	17.65	-0.52	8.67	15.84	6.31
TDH	12.33	15.23	-0.15	9.31	49.53	2.02
Flow_rate	0.24	0.29	-0.09	-0.14	78.80	1.27

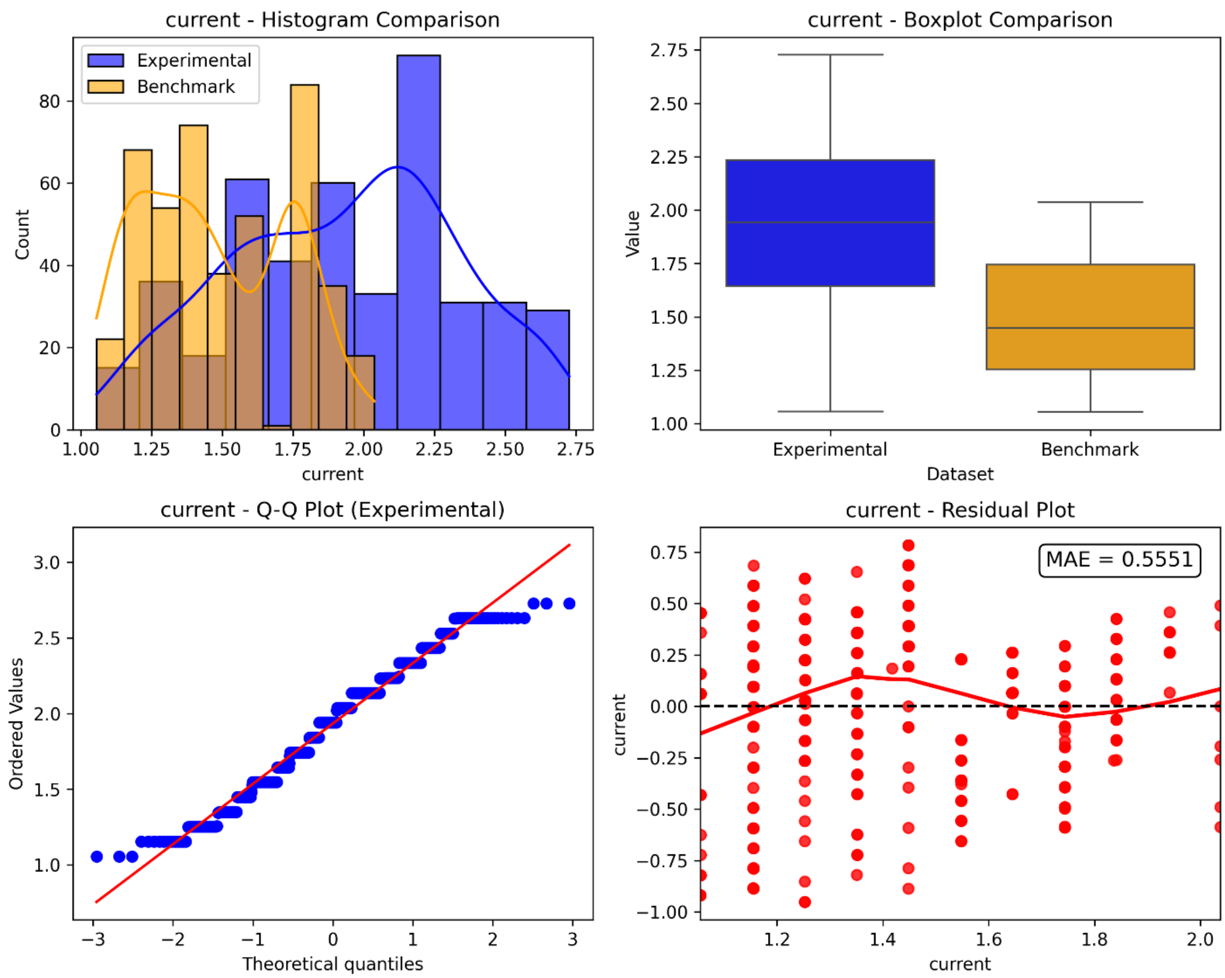

Figure 4 Statistical analysis of the current (experimental vs. benchmark)

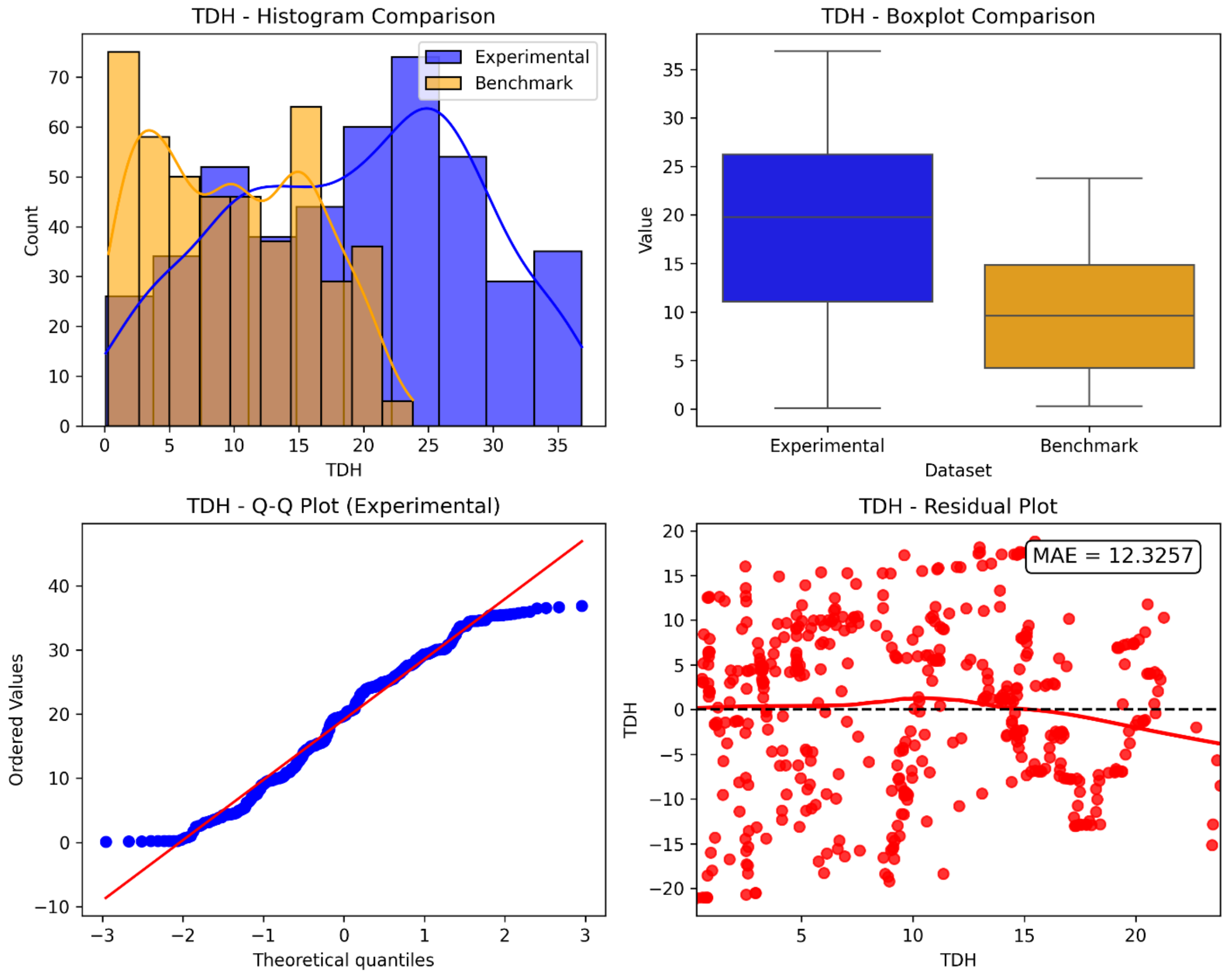

Figure 5 Statistical Analysis of the TDH (Experimental vs. Benchmark)

Based on statistical measurements and graphical illustrations (Figure 4 and Figure 5), we had the ability to give an in-depth assessment of the accuracy and reliability of each parameter as follows:

Accuracy assessment

Current

- MAE reached 0.56 and RMSE 0.70: Relatively low error values indicate excellent accuracy.
- Bias reached 0.46: Slight overestimation but not significant.

Voltage

- MAE reached 7.64 and RMSE 8.66: Average absolute difference between experimental and benchmark values, showing moderate accuracy.
- Bias reached -1.57: Notable negative bias indicates systematic underestimation.

Power Output (P_{out})

- MAE reached 14.63 and RMSE 17.65: Maximum absolute errors among the parameters indicate moderate accuracy.
- Bias reached 8.67: It means significant overestimation.

Total dynamic head (TDH)

- MAE reached 12.33, and RMSE 15.23: Substantial errors indicating moderate accuracy.

- Bias reached 9.31: Significant positive bias showing systematic overestimation.

Flow rate

- MAE reached 0.24, and RMSE 0.29: Low absolute errors suggest that the data show great accuracy with few deviations between benchmark and experimental values.
- Bias reached -0.14: Minimal bias suggesting limited systematic error.

Reliability assessment

Current

- CV reached 20.74%: Exceeds ideal threshold (which is <15%), indicating moderate variability relative to mean.
- SNR reached 4.82: Acceptable but not ideal SNR, approaching the minimum acceptable, which is equal to 5, which means acceptable variability.
- Correlation reached -0.24: Negative correlation, which indicates a weak inverse relationship between experimental and benchmark values.

Voltage

- CV reached 18.72 %, which is similar to the current variability.
- SNR reached 5.34: It is an acceptable signal-to-noise ratio above the minimum threshold.
- Correlation reached -0.52: Negative correlation suggests a weak relationship between experimental and benchmark data.

Power output (P_{out})

- CV reached 15.84%: It is just above acceptable variability.
- SNR reached 6.31: It is the best SNR among all parameters, showing higher reliability.
- Correlation reached -0.52: Strongest negative correlation.

Total dynamic head (TDH)

- CV reached 49.53%: Very high variability, indicating highly inconsistent measurements.
- SNR reached 2.02: Poor signal-to-noise ratio, suggesting measurements heavily affected by noise.

These results are due to flow measurements during the non-steady state.

- Correlation reached -0.15: Negative correlation suggesting moderate reliability.

Flow rate

- CV reached 78.80%: Extremely high variability, the worst among all parameters.
- SNR reached 1.27: Very poor signal-to-noise ratio, indicating measurements dominated by noise.
- Correlation (-0.09): Slight negative correlation, indicating poor reliability.

There seems to be logic because flow rate and TDH are hydraulically linked. When we change one of these parameters using the throttling valve, we affect the other one automatically.

Overall, the analysis of the metrics reveals varying levels of accuracy and reliability across the parameters, here's a concise summary:

- Flow_rate is the most accurate (lowest MAE and RMSE).
- P_out is the least accurate (highest MAE and RMSE).
- P_out als is the most reliable (highest SNR and lowest CV).
- Flow_rate is the least Reliable (highest CV and lowest SNR).

Total dynamic head (TDH) control

By utilizing a valve-throttling control mechanism, we successfully obtained the pump's TDH (Total Dynamic Head) over the course of a whole day. This approach allowed us to continuously monitor and adjust the pump's performance in response to varying conditions, especially changes in solar irradiance. The TDH curve demonstrates how the pump dynamically adapts to these fluctuations, providing a comprehensive understanding of its operational range. The maximum value of TDH at daytime is around 40 meters as indicated in Figure 6. The results are an important factor in establishing the performance and reliability of the pumping system under varying environmental conditions.

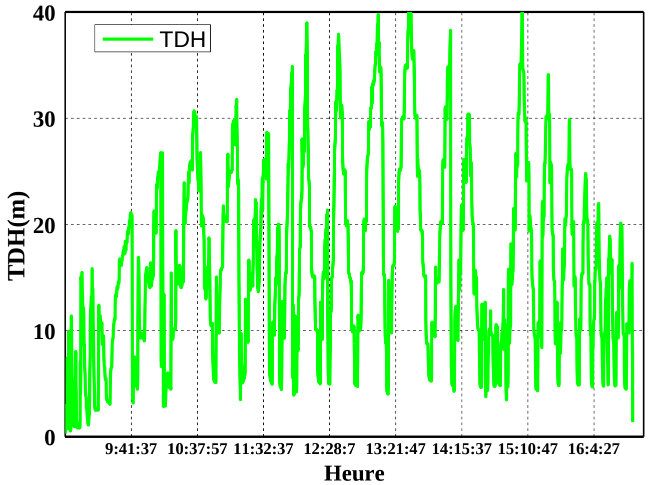

Figure 6 Daily variation of the TDH of the pump

We wait until 9:30 to reach the desired TDH (24.5 m). To increase the daily pumping duration and, consequently, the daily amount of water pumped. We used a buck converter, especially in the early morning and late evening (when there is low sunlight). Figure 6 shows that the pump cannot achieve the desired TDH at sunrise or sunset, unlike in the middle of the day. This is because the pump's characteristics depend on solar radiation (unstable during the day), which is quite natural in this kind of installation (pump installed along the sun).

Voltage and flow-rate characteristic

The flow rate and voltage curves of the select pump at sunrise without using a buck converter are summarized in the graph (Figure 7). For more analysis, we opted for a regression study to interpret the relationship between THD and voltage (Figure 8).

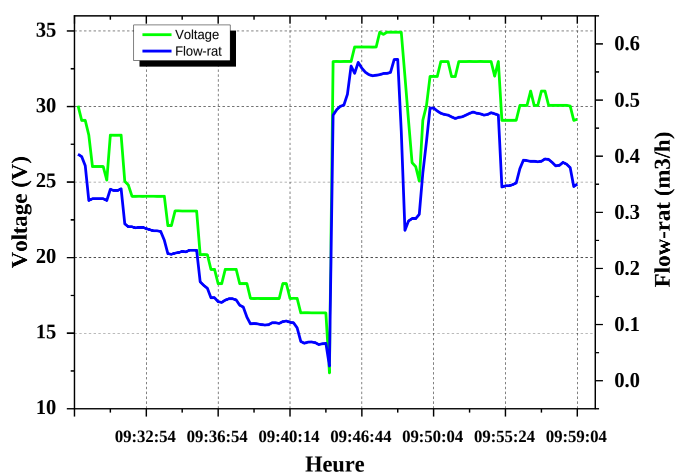

Figure 7 Flow rate –Voltage characteristics of the pump at sunrise

Figures 7 and 8 represent the relationship between the voltage from the solar generator and the flow rate. They are visually identical, which means that the flow rate is proportional to the pump's input voltage.

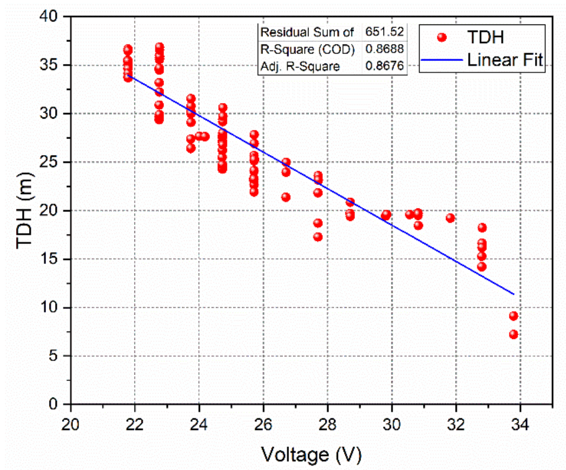

Figure 8. The scatter plot with a fit of flow rate versus Voltage

Characteristics of Current and TDH

Figures 9 and 10 summarize the pump's TDH-current characteristic curves at sunrise and sunset without using the buck converter. For more analysis, we use a regression study to interpret the relationship between current and THD (Figure 11).

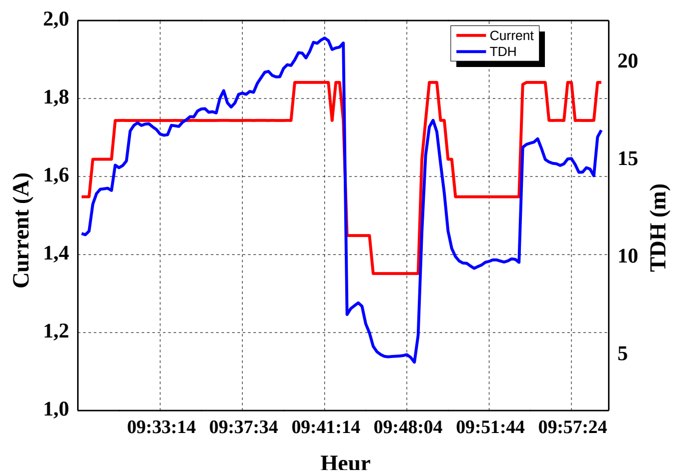

Figure 9 Characteristics of TDH and Current at sunrise without using the buck converter

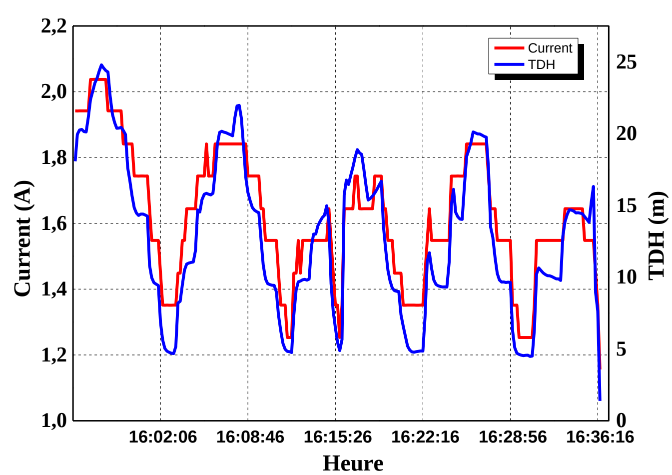

Figure 10 Characteristics of TDH and Current at sunset without using the buck converter

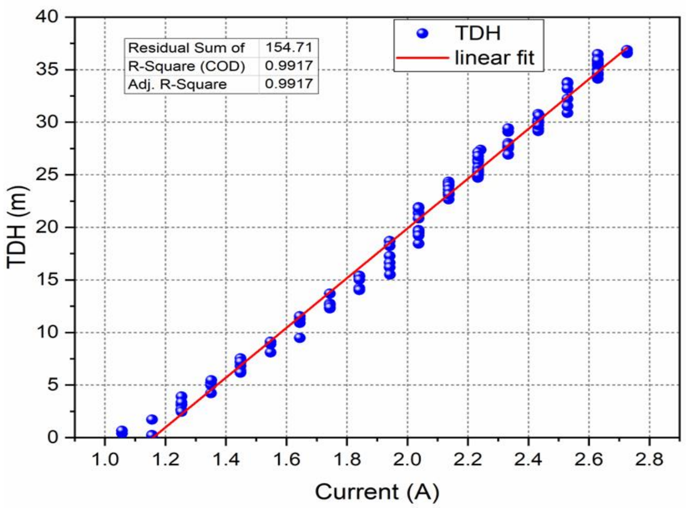

Figure 11 The scatter plot with a fit of TDH versus Current

Figures 9, 10, 11 and 12 allow us to conclude the following:

- The TDH of the pump is proportional to the input current.
- By using the buck converter, we can ensure that the pump can achieve the appropriate height of the head during sunrise and sunset, which you would not be able to do otherwise.

Characteristics of the Current and TDH of using the buck converter

Figure 12 and Figure 13 summarize the characteristics of TDH and current curves of the pump under sunrise and sunset with the use of the buck converter.

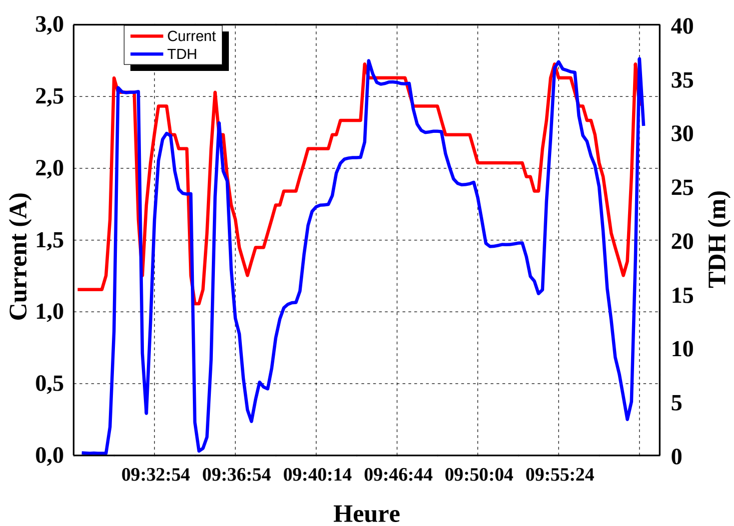

Figure 12 TDH –Current characteristics at sunrise using buck converter

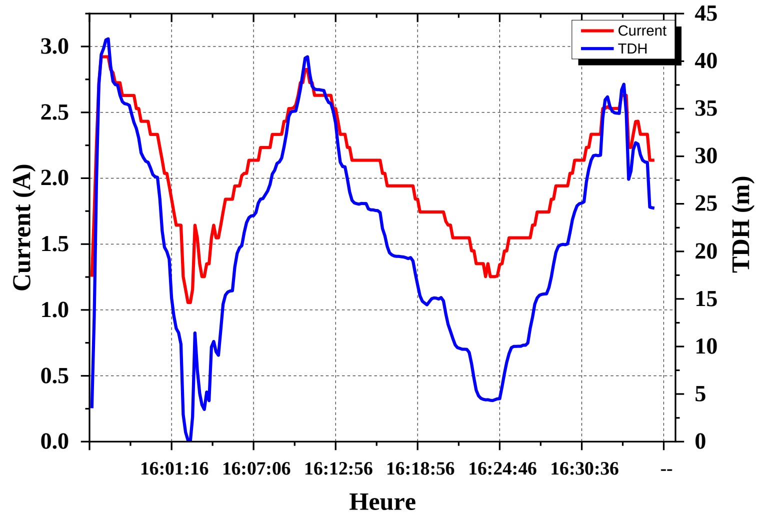

Figure 13 Characteristics of TDH and Current at sunset using the buck converter

Voltage conversion efficiency

The following equation defines the voltage conversion efficiency:

$$\text{Efficiency (\%)} = \frac{P_{Out}}{P_{in}} \times 100 \tag{4}$$

Where:

$P_{in} = V_{in} \times I_{in}$ and $P_{out} = V_{out} \times I_{out}$

The input parameters of the Buck converter are derived from the solar panel (voltage and current), while the output parameters are derived from the Buck converter itself. The results are displayed in Figure 14 and 15.

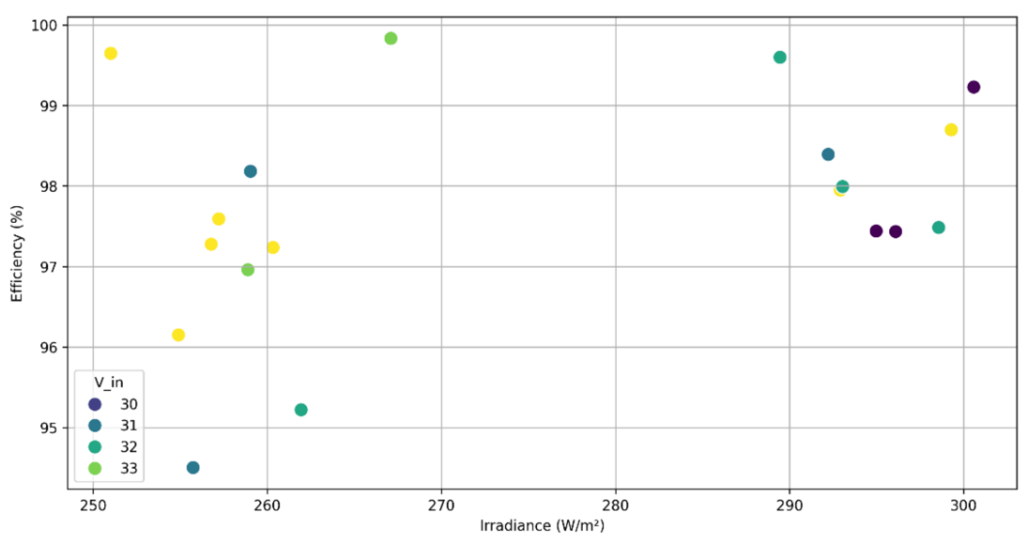

Figure 14 Efficiency vs Irradiance

- At low irradiance levels (251 to 260 W/m²), the efficiency is between 94.5% and 99.65% (97.2% average), demonstrating that performance is hardly influenced by low irradiance.
- At irradiance between 261 and 300 W/m², the efficiency varies between 95.2% and 99.83% (97.8% average), highlighting that the efficiency is always high.

The above results demonstrate the Buck converter's ability to reliably and efficiently transfer power from the solar panel to the water pump under these operating conditions.

Power stability of the Buck converter

We measured the system performance parameters to evaluate the buck converter's power stability. Table 5 summarizes the obtained results.

Table 5 Power and voltage stability metrics

Metric	Input	Output	Improvement (%)
Power fluctuation (w)	34.35	12.76	62.80
Relative power stability (%)	103.84	31.27	69.90
Voltage ripple (v)	24.46	16.94	31
Relative voltage ripple (%)	97.04	73.50	24

To prepare this table, we used the following equations:

Power Fluctuation

$$\Delta P_{\text{out}} = \max(P_{\text{out}}) - \min(P_{\text{out}}) \quad (5)$$

Relative Power Stability (%)

$$\left(\frac{\Delta P_{\text{out}}}{P_{\text{out}}}\right) \times 100 \quad (6)$$

Voltage Ripple (V)

$$\Delta V_{\text{out}} = \max(V_{\text{out}}) - \min(V_{\text{out}}) \quad (7)$$

Relative Voltage Ripple (%)

$$\left(\frac{\Delta V_{\text{out}}}{V_{\text{out}}}\right) \times 100 \quad (8)$$

The Buck converter demonstrates clear benefits in terms of power stability and voltage so regulation reducing power fluctuations by 62.8% and voltage ripple by 30.8%. Overall, the Buck converter improves the system performance under low irradiance conditions.

Behavior of buck converters during rapid solar irradiance transients

Figure 15 shows how solar irradiance and power output relate to each other over time, from around 9:28 AM until 10:01 AM, the morning period of our test. The blue zoom box highlights an area of particular interest: the buck converter's response to the big drop in irradiance. The buck converter can be observed adjusting operating parameters to maintain power output as efficiently as possible during this transition. The consistent power output observed during periods of fluctuating irradiance indicates that the buck converter is operating effectively near the maximum power point, even under varying conditions.

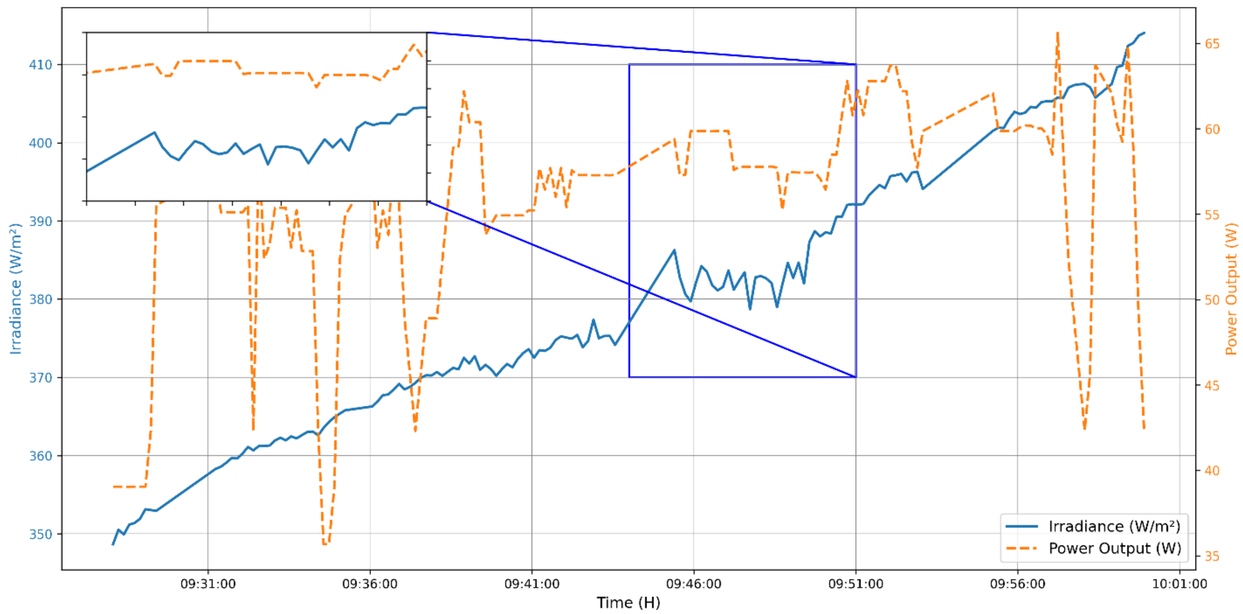

Figure 15. Analysis of solar irradiance and power generation

Dynamic response and electrical losses of the buck converter

Total losses

The total losses are calculated for each irradiance scenario; we used the following equations:

$$P_{\text{loss}} = P_{\text{int}} - P_{\text{out}} \quad (9)$$

The following is a breakdown of losses into ranges of irradiance (Table 6):

Table 6: Buck converter efficiency and power loss analysis across solar irradiance ranges

Irradiance range (w/m²)	Average Pin (w)	Average Pout (w)	P_{losses} (w)	Loss type
250–260	39.1	37.9	1.2	Conduction (moderate)
260–270	40.1	38.2	1.9	Conduction (higher)
280–290	43.2	42.3	0.9	Switching (higher)
290–300	44.2	43.5	0.7	Switching (lower)
300–310	42.1	41.8	0.3	Minimal (optimal efficiency)

It is evident from the above-provided information that:

- Power losses generally decrease with an increase in irradiance from 1.9W to 0.3W.
- The Input and output power typically rise with irradiance to level off at 290-300 W/m²
- The system has slightly reduced power handling at the highest irradiance range but with optimum efficiency

Correlation between v_{in} fluctuations and dynamic response

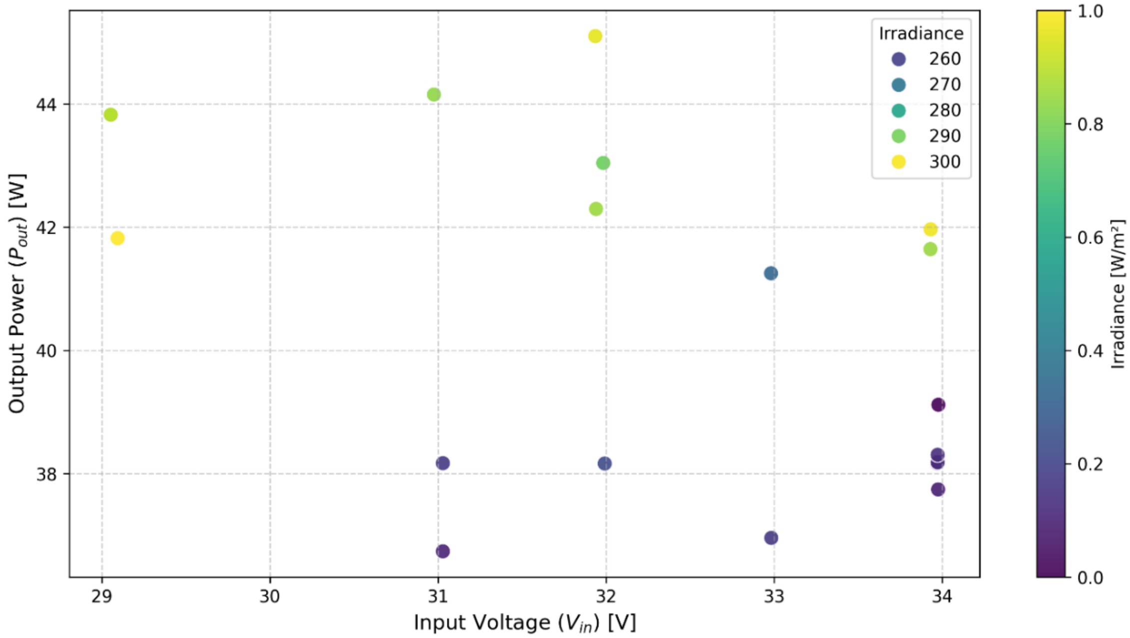

Figure 16 V_{in} vs P_{out}

Figure 16 shows that the graph of V_{in} and P_{out} seems to have a linear relationship at all irradiances. To validate this assumption, we employ Pearson correlation analysis.

The Pearson Correlation is given in the formula 2:
In our data, we call X=V_{in} and y =P_{out} where

$$\mathrm{Cov}(V_{\mathrm{in}}, P_{\mathrm{out}}) = \frac{1}{N-1}\sum_{i=1}^{N}\left(V_{\mathrm{in},i} - \overline{V_{\mathrm{in}}}\right)\left(P_{\mathrm{out},i} - \overline{P_{\mathrm{out}}}\right) \quad (10)$$

$$\sigma_{V_{\mathrm{in}}} = \sqrt{\frac{1}{N-1}\sum_{i=1}^{N}\left(V_{\mathrm{in},i} - \overline{V_{\mathrm{in}}}\right)^2} \quad (11)$$

$$\sigma_{P_{\mathrm{out}}} = \sqrt{\frac{1}{N-1}\sum_{i=1}^{N}\left(P_{\mathrm{out},i} - \overline{P_{\mathrm{out}}}\right)^2} \quad (12)$$

After application of the formulas to our data: $r = -0.469 \ (p - value) < 0.05)$

This indicates a negative correlation between V_{in} and P_{out}, indicating that an increase in one of them is usually matched by a decrease in the other. As a dynamic response, the converter adjusts V_{in} to maximize P_{out} under varying irradiance.

Table 7 Comparison of DC-DC converter efficiencies for PV systems under low irradiation conditions

Reference	**Rated power (W)**	**Type of converter**	**System efficiency for low irradiation (%)**
(Hmidet A et al., 2015)	610	Boost	95.2 (for 400 w/m^2)
(Kumar R et al., 2015)	4400	Boost-Buck (BB)	78 (for 200 w/m^2) 80.6 (for 300 w/m^2)

(Caracas JV et al.,2013)	210	Two Inductor Boost Converter (TIBC)	93.64 (max)
(Mishra & Singh, 2018)	875	Dual output Zeta derived DC-DC	67 (for 200w/m^2) 72 (for 300w/m^2)
(Singh & Mishra,2019)	875	Dual-Output (SIDO) Buck–Boost	67 (for 200w/m^2) 70.2 (for 300w/m^2)
Present study	100	Buck	97.2% (from 250 to 261w/m^2 97.8% (from 261 to 300w/m^2)

The table 7 shows the results of previous studies similar to our study. We notice a large variation in results between different studies (from 67 % to 97 %) regarding the system's behavior under weak solar radiation conditions (from 67 % to 97 %) . This variation is due to factors including the total rated power, the type of converter, and the conversion method. However, our study shows a significant advantage over other studies.

TDH improvement

Figures 17 and 18 compare the pump's TDH with and without the use of a buck converter at sunrise and sunset. They also show a comparison between the reach TDH with and without the adoption of a buck converter. The maximum TDH obtained without using the buck converter is approximately 20 m; in contrast, it can easily reach 40 m with the buck converter. The pump's TDH is higher when employing a buck converter than when it is not used.

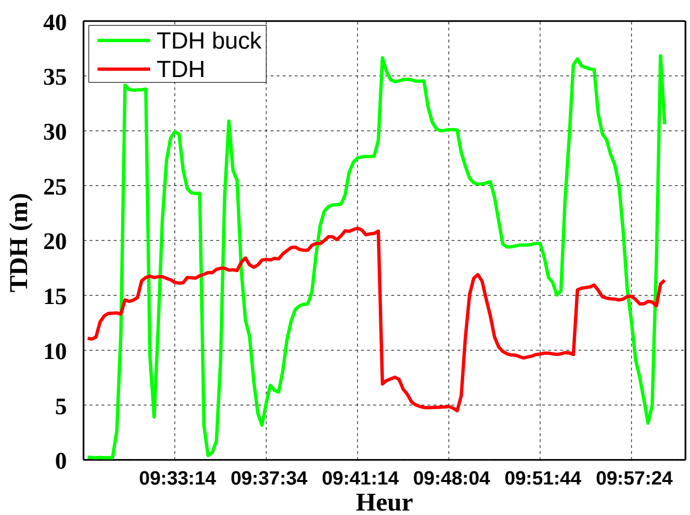

Figure 17 TDH characteristic of the pump at sunrise

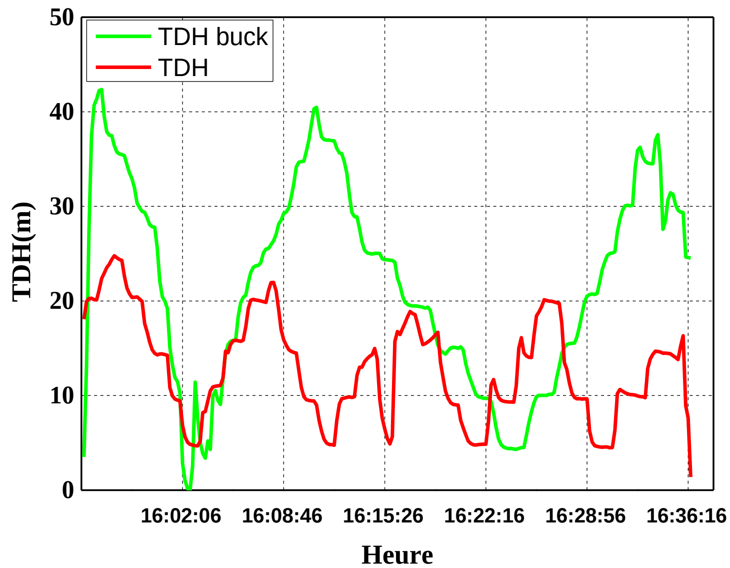

Figure 18 TDH characteristic of the pump at sunset

5. CONCLUSIONS

In this paper, we have carried out the laboratory performance testing of a solar pump (SHURflo 9325) under low irradiation. Statistical analysis of data shows different levels of accuracy and reliability of the parameters. What has been confirmed to us is that TDH needs significant enhancements. The results indicated that the pump was unable to achieve the desired Total Dynamic Head (TDH) during sunrise and sunset periods, when solar irradiance levels were low. We used a buck converter to overcome this issue. The results demonstrated that the buck converter influences the TDH and pump flow, especially with fluctuating PV input power. Because it is built to maximize the current provided to the pump motor, TDH is seen to increase significantly around sunrise and sunset.

The Buck converter significantly improves power stability and voltage regulation through the reduction of power oscillations by 62.8% and voltage ripple by 30.8% through its dynamic switching control and feedback. It works better in renewable energy systems like photovoltaic systems at low irradiance levels, with stable output and shielding devices from voltage volatility. It enhances system performance, energy efficiency, and reliability under fluctuating conditions.

There was, however, a noticeable decrease in flow caused by the relaxation of voltage following the heightened current of the converter. A pump that is designed to operate on a sun-running principle, therefore, performs more optimally with the incorporation of a buck converter. But the benefits are mostly achieved under extraordinary circumstances, such as at sunrise, sunset, and during the start-up time of the pump.

From this work's perspective, several designs have been improved to enhance the efficiency of a buck converter in low-irradiance conditions for solar water pumping systems. Key improvements include integrating MPPT controllers with sensor less motor control to optimize power extraction and adjust pump speed dynamically. Hybrid energy storage (e.g., supercapacitors). These strategies address variable irradiance challenges, motor surge currents, and harsh operating conditions, ensuring efficient water delivery even in low-light scenarios.

Nomenclature

DC	Direct current
E	solar radiation, w/ m^2
I_{in}	Input current, A
I_{sc}	Short circuit current
I_{out}	Output current, A
MOSFET	Metal oxide semiconductor field effect transistor

MPPT	Maximum Power Point Tracking
muIsc	Temperature coefficient for Isc, mA/°C
PV	Photovoltaic
P_{out}	Output power, w
P_{out}	Mean P_{out}
P_{in}	Input power, w
Q	Flow rate, m^3/h
r	Pearson correlation coefficient
Sdt	Standard deviation
TDH	Total dynamic head, m
VDC	voltage of a direct current
V_{in}	Input voltage, v
$\overline{V_{in}}$	Mean V_{in}, v
VOC	Open circuit voltage
V_{out}	Output voltage, v
x	Data point
μ	Mean of data set
μ_x	Mean of x data set
μ_y	Mean of y data set
σ	Standard deviation
σ_{Vin}	Standard deviation of V_{in}
σ_{Pout}	Standard deviation of P_{out}

Acknowledgements

We would like to thank the participants, whose input was crucial in enabling this research analysis. We also thank our institutions for providing us with various resources, such as laboratories and study materials.

Author Contributions

All authors contributed to the study conception and design, Conceptualization: H. AMMAR and N. BENBAHA, Methodology: H. AMMAR and N. BENBAHA, Software: H. Ammar, Validation: H. AMMAR and N. BENBAHA, Visualization: H. AMMAR, Investigation: N. BENBAHA, Writing – original draft: H. AMMAR, Formal analysis: H. AMMAR and N. BENBAHA, Supervision: MT. BOUZIANE. All authors have read and agreed to the published version of the manuscript.

Ethical issues

Not applicable.

Informed consent

Not applicable.

Funding

This study has not received any external funding.

Conflict of Interest

The author declares that there are no conflicts of interest.

Data and materials availability

All data associated with this study are presented in the paper.

REFERENCES

1. Alkuhayli A, Noman AM, Al-Shamma'a AA, Abdurraqeeb AM, Alharbi M, Hussein Farh HM, Qamar A. Enhancing photovoltaic-powered DC shunt motor performance for water pumping through fuzzy logic optimization. Machines. 2024;12(7):442. doi: 10.3390/machines12070442
2. Ammar H, Bouziane MT, Bakelli Y. L'influence de la variation de débit sur les performances d'une pompe solaire. Revue des Energies Renouvelables SIENR. 2012;12:23-8.
3. Ammar H, Bouziane MT, Boukebbous S, Benbaha N, Boutadara A. Point de fonctionnement d'une pompe solaire installée au fil du soleil au labo. In2ème conférence Internationale des énergies renouvelables CIER-2014 International Journal of Scientific Research & Engineering Technology (IJSET) 2014; 3:10-14.
4. Angadi S, Yaragatti UR, Suresh Y, Raju AB. Comprehensive review on solar, wind and hybrid wind-PV water pumping systems-an electrical engineering perspective. CPSS Transactions on Power Electronics and Applications. 2021;6(1):1-19. doi: 10.24295/cpsstpea.2021.00001
5. Benbaha N, Zidani F, Nait-Said MS, Zouzou SE, Boukebbous S, Ammar H. DSPACE validation of improved backstepping optimal energy control for photovoltaic systems. In 2018 6th International Renewable and Sustainable Energy Conference (IRSEC). IEEE. 2018; 1-6.
6. Caracas JV, de Carvalho Farias G, Teixeira LF, de Souza Ribeiro LA. Implementation of a high-efficiency, high-lifetime, and low-cost converter for an autonomous photovoltaic water pumping system. IEEE Transactions on Industry Applications. 2013; 50(1):631-41.
7. Crovella T, Paiano A, Falciglia PP, Lagioia G, Ingrao C. Wastewater recovery for sustainable agricultural systems in the circular economy–A systematic literature review of Life Cycle Assessments. Science of The Total Environment. 2024; 912:169310.
8. Durga N, Schmitter P, Ringler C, Mishra S, Magombeyi MS, Ofosu A, Pavelic P, Hagos F, Melaku D, Verma S, Minh T. Barriers to the uptake of solar-powered irrigation by smallholder farmers in sub-saharan Africa: A review. Energy Strat Rev. 2024; 51:101294. doi: 10.1016/j.esr.2024.101294
9. Farhat M, Barambones O. Advanced Control Scheme Optimization for Stand-Alone Photovoltaic Water Pumping Systems. Computation. 2024;12(11):224. doi: 10.3390/computation12110224
10. Girgis ME, Elkhateeb NA. Enhancing photovoltaic MPPT with P&O algorithm performance based on adaptive PID control using exponential forgetting recursive least squares method. Renew Energy. 2024; 237:121801. doi: 10.1016/j.renene.2024.121801
11. Haque A. Maximum power point tracking (MPPT) scheme for solar photovoltaic system. Energy Technol Policy. 2014;1(1):115-22. doi: 10.1080/23317000.2014.979379
12. Hmidet A, Rebei N, Hasnaoui O. Experimental studies and performance evaluation of MPPT control strategies for solar-powered water pumps. In 2015 Tenth international conference on ecological vehicles and renewable energies (EVER). IEEE. 2015; 1-12.
13. Kassakian JG, Perreault DJ, Verghese GC, Schlecht MF. Principles of power electronics. Cambridge University Press; 2023.
14. Kumar CM, Singh S, Gupta MK, Nimdeo YM, Raushan R, Deorankar AV, Kumar TA, Rout PK, Chanotiya CS, Pakhale VD, Nannaware AD. Solar energy: A promising renewable source for meeting energy demand in Indian agriculture applications. Sustain Energy Technol Assessments. 2023; 55:102905. doi: 10.1016/j.seta.2022.102905
15. Kumar R, Singh B, Chandra A, Al-Haddad K. Solar PV array fed water pumping using BLDC motor drive with boost-buck converter. In 2015 IEEE Energy Conversion Congress and Exposition (ECCE). IEEE 2015; 5741-5748.
16. Liou WR, Yeh ML, Kuo YL. A high efficiency dual-mode buck converter IC for portable applications. IEEE Trans Power Electron. 2008;23(2):667-77. doi: 10.1109/tpel.2007.915047
17. Mishra AK, Singh B. Design of solar-powered agriculture pump using new configuration of dual-output buck–boost converter. IET Renewable Power Generation. 2018;12(14):1640-50.
18. Muralidhar K, Rajasekar N. A review of various components of solar water-pumping system: Configuration, characteristics, and performance. Int Trans Electr Energy Syst. 2021;31(9):e13002. doi: 10.1002/2050-7038.13002
19. Nisha R, Sheela KG. Review of PV fed water pumping systems using BLDC. Motor. Mater Today. 2020; 24:1874-81. doi: 10.1016/j.matpr.2020.03.612

20. Raj A, Arya SR, Gupta J. Solar PV array-based DC–DC converter with MPPT for low power applications. Renewable Energy Focus. 2020;34:109-19.
21. Ramli RM, Jabbar WA. Design and implementation of solar-powered with IoT-Enabled portable irrigation system. Internet of Things and Cyber-Physical Systems. 2022; 2:212-25.
22. Singh B, Mishra AK. Performance analysis of a solar-powered water pumping using improved SIDO buck–boost converter. IET Power Electron. 2019;12(11):2904-11. doi: 10.1049/iet-pel.2018.5448
23. Sutikno T, Samosir AS, Aprilianto RA, Purnama HS, Arsadiando W, Padmanaban S. Advanced DC–DC converter topologies for solar energy harvesting applications: a review. Clean Energy. 2023;7(3):555-70.